Isotope and Pressure Effects on Liquid–Liquid Equilibria in Polymer Solutions. H/D Solvent Isotope Effects in Acetone–Polystyrene Solutions

Jerzy Szydlowski† and W. Alexander Van Hook*

Chemistry Department, University of Tennessee, Knoxville, Tennessee 37996-1600

Received July 26, 1990; Revised Manuscript Received April 15, 1991

ABSTRACT: Cloud point and spinodal data are reported for some polystyrene–acetone and polystyrene–methylcyclopentane solutions as functions of pressure, molecular weight, and (for acetone) solvent H/D fraction. The H/D isotope effects on the coexistence curves and their pressure dependences are both large. An increase in pressure or a change in substitution from D to H increases the region of miscibility. The results are discussed in the context of current ideas of polymer solutions as modified by the theory of isotope effects in condensed phases.

Introduction

Investigations of isotope effects (IE's) on the physical properties of condensed phase molecules,[1,2] including IE's on phase equilibria, combined with information on the variables governing phase separation in the parent system,[3] can contribute significantly to knowledge of the nature of such solutions, including understanding at the molecular level.[1-3] Isotope theory develops expressions for the thermodynamic properties of liquids and solutions in terms of the atomic and molecular motions on a multidimensional potential energy surface (PES). Properly defined PES's are invariant to isotope substitution (within the validity of the Born–Oppenheimer approximation), and it follows that IE's on observed properties, like the excess free energy, can be employed to test a PES modeling the solution. Cloud points, binodal and spinodal loci, and many other parameters used to describe phase equilibria are sensitive functions of PES. Thus combining measurements of IE's with other kinds of thermodynamic information, and with spectroscopic data, can lead to appreciable refinement in our knowledge of the PES describing the system. It is in this context that we decided to initiate a program to make accurate high-precision measurements of the temperature, pressure, molecular weight, and isotope dependence of miscibility in polymer–solvent solutions and have recently reported on new equipment for that purpose.[4] The present paper outlines methods for interpretation of isotope effects in polymer phase equilibria.

Another reason to investigate thermodynamic IE's in polymer–polymer and polymer–solvent solutions comes from their widespread use in neutron scattering investigations. Sensitivity and contrast can be controlled by varying H/D ratios, but this complicates interpretation unless one makes the too common assumption of neglecting thermodynamic isotope effects and regards the deuterium label as a simple tracer. Wignall[5] has recently reviewed neutron scattering in polymer systems. Other reviews are available.[6-8] Deviations from the simple "tracer" approximation became apparent in the mid-1970s. Thus Strazielle and Benoit[9] found Θ temperatures of polystyrene (PS)–cyclohexane solutions to be markedly influenced by deuterium substitution on either solvent or polymer or both. Kirste et al.[10] Stein and co-workers,[11] Aitkin et al.[12] and Lin et al.[13] reported IE's on the temperature of phase separation in polymer blends. None of the above studies reported phase equilibrium data at high precision. Neither have any of the studies been interpreted using the theory of isotope effects in condensed phases.[1,2]

A striking example of the contribution of thermodynamic IE's to nonideality was the recent observation of phase separation in binary solutions of isotopes (no third component). Bates and Wignall have reported demixing in solutions (blends) of protio and deuterio polystyrenes[14] and protio and deuterio polybutadienes.[15] They have presented an interpretation of the physical origin of the demixing;[16] an independent and somewhat different interpretation has been given by Singh and Van Hook.[17] The latter authors applied their general theory of excess thermodynamic properties in mixtures of isotopes[18] to the case of polymer–polymer solutions. Previous to the Bates–Wignall observations, phase separation in mixtures of isotopes had not been observed except in quantum fluids at very low temperature.[19]

Quantitative interpretation of IE's on phase equilibria in polymer–polymer and polymer–solvent solutions is (will be) facilitated by comparisons with extant work on small-molecule systems. The early literature has been reviewed by Rabinovitch[20] and Khurma et al.[21] Recently Singh and Van Hook[22] and Salvi and Van Hook[23] have made measurements of solute and solvent H/D effects for methanol–cyclohexane and ethylene glycol–nitromethane solutions, respectively. The demixing curves and their IE's were analyzed quantitatively.[1,2,22] In the analysis the authors selected an extended mean field expression for the dependence of the excess free energy (and its IE) on temperature, pressure, and composition, including the immediate region of the temperature of critical demixing, T_c or T_c' (the prime denotes the lighter isotope). Higher order terms in the free energy expression serve to broaden the spinodal and binodal surfaces and yield a value for $\beta_{phen} \approx 1/3$ (eq 1, below). It is important to keep in mind, however, that modern theories of critical phenomena, including scaling theories,[24] predict logarithmic singularities at the critical point. In the region of arbitrary closeness to T_c, the various thermodynamic phenomena can be described by a set of universal scaling exponents. Not too far from T_c the coexistence line for liquid–liquid equilibria can be written

$$|x^* - x^{**}| = A(1 - T/T_c)^\beta = At^\beta \qquad (1)$$

where x^* and x^{**} are concentrations of coexisting phases,

* Author to whom correspondence should be addressed.
† On leave at the University of Tennessee 1988–1990. Permanent address: Chemistry Department, University of Warsaw, Zwirki i Wigury 101, 02-089 Warsaw, Poland.

0024-9297/91/2224-4883$02.50/0

t is the reduced temperature as defined in the equation, A is a system-specific amplitude parameter, and β is a universal scaling exponent known theoretically and experimentally to be 0.325 ± 0.003. A difficulty arises because in the limit of arbitrary closeness to T_c any mean field representation predicts $\beta = 0.5$ and therefore is incorrect in the limit $T \rightarrow T_c$ ($t \rightarrow 0$). Since condensed-phase IE theory is a mean field theory, it cannot be accurately applied in that limit. The difference in the limiting values of β for mean field and β for scaling theory arises because the mean field approach does not properly consider the long-range concentration fluctuations found near T_c. However, at some small distance from $t = 0$ (denoted as the Ginzburg limit, t_g), fluctuations are damped out, the system returns to the mean field domain, and it is once again useful to employ analytic representations of the free energy. Gordon and Torkington[25] and Singh and Van Hook[26] (SVH) have considered mean field versus nonclassical representations from different points of view. SVH, in agreement with other workers,[27] conclude that the range of nonclassical effects fit by the asymptotic theory extends to $t_g \approx 10^{-3}$, some argue even less.[25] At $T_c = 300$ K this amounts to $(T_c - T) = 0.3$ K, or less. We conclude, and it is a conclusion of some importance, that mean field analysis of demixing curves is appropriate over most of the phase diagram. Parenthetically we expect fitting errors caused by misapplication of mean field analysis to data nets that include points within t_g to decrease as that limit narrows.

In spite of the limitations of mean field theory in the critical region, its application to polymer critical phenomena has been widespread. This is partly a consequence of the fact that scaling theory makes no prediction of the location of T_c or the amplitudes of the demixing curve but only predicts the shape of the curve in the vicinity of the critical point. Mean field theories, on the other hand, allow one to write analytic expressions for T_c and A (eq 1) using just those parameters that define the free energy surface. With an extended theory properly incorporating higher order terms the expression for the demixing surface can be broadened to accurately represent experimental observation at all temperatures except those *very* close to T_c. Thus, recently, in addition to work cited above,[25-27] Scott and co-workers have used an extended classical free energy expression to describe tricritical phenomena in polystyrene and small molecule solutions, de Pablo and Prausnitz[29] employed extended classical expressions and revised scaling to include the critical region in thermodynamic calculations, and Carvolli et al.[30] and Stroeks and Niss[31] use classical theories to predict polymer phase equilibria in good agreement with experiment. Also earlier Koningsveld et al.[32] and Irvine and Gordon[33] described a mean field two-phase theory that they claim adequately models phase separation to within 0.015 K of T_c. They[32] comment that nonclassical scaling theories will need extension to deal with polydispersity. It is not our intention here to survey the enormous recent literature detailing the application of thermodynamic theory to polymer solutions in order to give a detailed exposition of the controversy under discussion. For polystyrene non (first order) mean field curvature is well established,[34] $\beta_{obs} = 0.32$, and is in good agreement with the theoretical nonclassical value. Even so, extended mean field theories (for example, the symmetrical mixture theory of Guggenheim,[35] extensions of simple Flory–Huggins theory,[36] and other approaches) can be applied over most of the range of experimental interest and reproduce the experimentally observed shape of the immiscibility curves well. Such fits admittedly do not focus on the limiting behavior as $T \rightarrow T_c$, but that is only important in a practical sense if the bulk of the data under discussion are extremely close to T_c, i.e., are substantially inside the Ginzburg limit. For broader data nets extended mean field theories are appropriate; it is in this spirit that the analysis below, which couples Guggenheim symmetrical mixture theory (a simple extension of regular solution theory) with the statistical theory of condensed phase isotope effects,[1,2] is offered. In such a calculation the shape and position of the immiscibility curves and their isotope effects are employed to make theoretically meaningful statements concerning the effects of temperature, pressure, isotope substitution, etc. on the free energy and then on the PES describing the intermolecular interactions in the solution.

Table I
Characteristics of Polystyrene Samples

sample	M_w (size excl)	M_n (viscosity)	M_w/M_n	source[a]
PS-25	2510	2730	<1.10	PC 61223
PS-40	4140	4080	<1.06	PC 30525
PS-55	5770	5670	<1.05	PC 50828
PS-80	8000	9100	<1.09	PC 80314
PS-130	13500	12900	<1.06	PC 30420
PS-50	5110		<1.07	SP 578-02
PS-75	7820		1.19	SP 579
PS-115	11500		1.07	SP 297

[a] PC = Pressure Chemical, Pittsburgh, PA; SP = Scientific Polymer Products, Ontario, NY. MW data provided by manufacturer.

In addition to the concentration dependence of the liquid–liquid equilibrium lines, the pressure dependence is also of interest. Thermodynamics expresses the pressure coefficient of the spinodal temperature, T_{sp}, as the ratio of second derivatives of mixture volume to entropy[36,38]

$$(dT/dP)_{sp} = (\partial^2 V/\partial \xi^2)_{sp}/(\partial^2 S/\partial \xi^2)_{sp} \qquad (2)$$

where ξ is an appropriate concentration scale and subscript "sp" denotes restriction to the spinodal surface. At the critical point $T_{sp} = T_c$. The volume dependence of the Helmholtz free energy is $-P$, the second derivative is the volume-weighted compressibility, and introduction of these relations leads to several convenient equations. The appearance of an upper demixing branch (showing a lower critical solution temperature (LCST)), is often associated with large compressibility effects.[36] Isotope effects on $(dT/dP)_c$ are small or zero for the UCST curve of small-molecule systems[22,23] because the IE on T_c itself is primarily associated with shifts in high-frequency internal vibrational modes.[22,39] LCST, on the other hand, is associated with low-frequency motions and expected to be more sensitive to pressure[36] and more isotope dependent. Siow et al., Zeman and Patterson,[41] and Saeki et al.,[42] have reported $(dT/dP)_c$ for UCS and LCS branches of some polystyrene solutions (but for protiated samples only) and have indicated a possible rationalization using the corresponding-states theories of Flory[43] or Patterson.[44]

Experimental Results

The data reported and/or discussed in this paper fall into two classes. In the first, low-precision visual determinations of cloud point curves (CPC's) were made, usually in sealed capillaries, for the purpose of mapping out the gross feature of the phase diagrams of interest; in the second, high-precision light scattering measurements of CPC's and spinodal loci were determined as functions of pressure and isotopic label by using apparatus and techniques described by Szydlowski et al.[4]

In reporting thermodynamic data on polymer solutions it may be convenient to employ either weight fraction or

volume fraction, φ, concentration scales. In comparing IE's an unmodified weight fraction scale is inappropriate (isotopically different solutions of identical mole fraction will be of different weight fractions). Using subscripts "1" and "2" to denote the low molecular weight solvent and polymer fractions, respectively, we define the W' scale as

$$W_2' = \frac{g_2(M_2'/M_2)}{g_2(M_2'/M_2) + g_1(M_1'/M_1)}$$

$$W_1' = \frac{g_1(M_1'/M_1)}{g_2(M_2'/M_2) + g_1(M_1'/M_1)} \quad (3)$$

Here g_1 and g_2 are the mass of components 1 and 2 in the solution, M_1' is the mean molar mass of the protio-substituted solvent, and M_1 is the molecular weight of the solvent of interest, M_2 and M_2' similarly denote the mean molar masses of the solute (but this paper reports no measurements with deuterated solute, so $(M_2'/M_2) = 1$ throughout). Of course for the solute the molecular weight distribution is infinitly sharp and molar mass and mean molar mass are one and the same. Notice that W_2' and W_1' are identical with the conventionally defined weight fraction (W_1, W_2) scale for the protio solutions but are (H/D) molecular mass weighted for deuterio solutions. It will sometimes be convenient to use the volume fraction (φ) scale defined by eq 4, ρ_1° is the density of the protio or

$$\varphi_2 = \frac{g_2/\rho_2^\circ}{g_1/\rho_1^\circ + g_2/\rho_2^\circ} \qquad \varphi_1 = \frac{g_1/\rho_1^\circ}{g_1/\rho_1^\circ + g_2/\rho_2^\circ} \quad (4)$$

deuterio solvent calculated from the data of Salvi and Van Hook[23] for acetone or Ye and Van Hook[45] for methylcyclopentane and ρ_2° is the density of pure liquid polymer as extrapolated to the temperature of interest following Hoecker et al.[46]

Materials. Polystyrenes of well-defined molecular weight and molecular weight distribution as obtained from Chemical Pressure Co. or Scientific Polymer Products Co. are listed in Table I together with the supplier's specifications. Solutions of room-temperature vacuum-dried polymer were made up gravimetrically. Acetone (Fisher CP), deuterioacetone (Merck), and methylcyclopentane (MCP) (Aldrich) were distilled at high reflux in a spinning band column. The collected fractions were carefully dried following the method of Chan and Van Hook[47] (acetone) or with molecular sieve or sodium (MCP). Phase transition temperatures are hypersensitive to water impurity and it is important to ensure complete drying.[38,48] Our measurements for acetone solutions give 4.5 mK/(ppm H_2O) for $dT_{UCS}/d\xi(H_2O)$ and 0.05 mK/(ppm H_2O) for MCP.

Preliminary Measurements, Low Precision. Cloud point data from sealed capillary measurements on polystyrene–$(CH_3)_2CO$ solutions (2500 Da < MW < 13 000 Da) are reported in Table II, part a, and diagrammed in Figure 1 for both the UCS and LCS branches. Similar data are presented for PS–MCP solutions in Table II, part b. The phase equilibrium data for the protio solutions are in reasonable agreement with earlier work.[40-42] Some pressure coefficients are also reported in Table II. Figure 2 demonstrates a typical set of measurements of the pressure dependence of the phase transition. Values of $(dT_{cp,max}/dP)$ are markedly different for the UCS and LCS branches and are also markedly different for different solvents (acetone versus MCP).

Table II
Cloud Points for Polystyrene Solutions[a]

W_1'	T_{upper}, K	T_{lower}, K	$-(dT/dP)_{upper}$, K·MPa^{-1}	$-(dT/dP)_{lower}$, K·MPa^{-1}
a. Polystyrene–$(CH_3)_2CO$ Solutions				
PS-25				
0.04	228	485		
0.10	230	483		
0.11	232	480		
0.14	231	482		
0.18	227	486		
0.225	225	488		
PS-50				
0.04	245	461		
0.11	258	451		
0.13	263	449		
0.18	261	448		
0.225	259	449		
PS-75				
0.04	264	446		
0.10	268	443		
0.11	269	440	1.30 $(CD_3)_2CO$	
0.13	270	438		
0.16			1.26 $(CD_3)_2CO$	
0.18	271	438		
0.20			1.10 $(CH_3)_2CO$	
0.225	267	438		
PS-115				
0.04	263	426		
0.10	270	419		
0.11	272	420		
0.14			1.32 $(CD_3)_2CO$	
0.13	272	421		
0.18	273	421		
0.225	272	422		
0.24			1.37 $(CD_3)_2CO$	
PS-130				
0.05	280	407		
0.10	284	404		
0.15	289	396		
0.18	287	398		
0.19			1.70 $(CH_3)_2CO$	
0.20			1.75 $(CH_3)_2CO$	-6.53 $(CH_3)_2CO$
0.23			1.76 $(CH_3)_2CO$	
0.25	284	404		
b. Polystyrene–c-$CH_3C_5H_9$ Solutions				
PS-25				
0.05	250	525		
0.10	255	518		
0.20	254	509		
0.25	252	507		
0.30	248	516		
PS-50				
0.05	262	507		
0.10	267	500		
0.15	269	499		
0.20	267	501		
0.25	267	502		
PS-75				
0.05	271	499		
0.10	272	495		
0.15	270	493		
0.20	270	491		
0.25	271	493		
PS-115				
0.05	291	489		
0.092			0.22	
0.10	294	484		
0.125	295	481		
0.14			0.26	
0.15	294	480		
0.20	294	480		
0.25	292	481		

[a] Visual determination in sealed capillaries.

Solvent isotope effects on demixing for UCS and LCS are reported in Table III. We estimate precision of these preliminary measurements as ±0.3 to ±0.5 K. IE's on

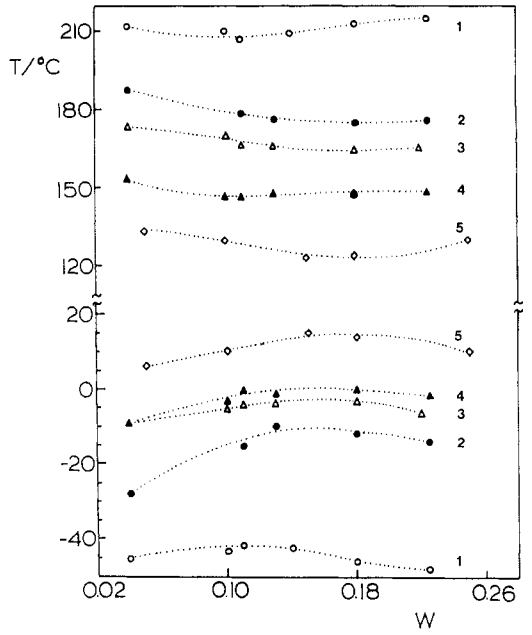

Figure 1. Plots of visually determined cloud point temperatures for polystyrene–$(CH_3)_2CO$ solutions contained in sealed capillaries. The abscissa, W, is the weight fraction of polymer. These data are referred to in the text as "low precision" and serve to map out the principal features of the phase diagram. The pressure over each sample is the solution vapor pressure. The labels on the solutions correspond to those in Table I. 1 (○) = PS-25; 2 (●) = PS-50; 3 (△) = PS-75; 4 (▲) = PS-115; 5 (◇) PS-130.

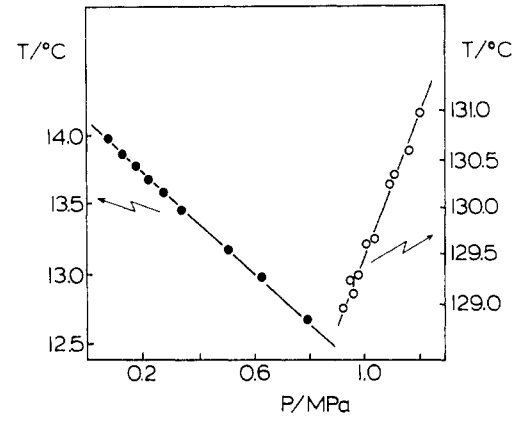

Figure 2. Effect of pressure on upper and lower cloud points in a polystyrene–$(CH_3)_2CO$ solution ($W_1 = W_1' = 0.20$ PS-130). The phase transition was determined by observing the changes in transmitted light and the data are of the type labeled low precision in the text. (●) Upper branch (UCS), experimental points; (○) lower branch (LCS), experimental points.

both UCS and LCS are large, on the order of 20 K or so, and increase with molecular weight. Since the high-precision apparatus[4] is capable of detecting the transition temperature the nearest 0.01 K, we conclude the method is a sensitive probe for the free energy surface, i.e., with a relative precision of a few parts per thousand. Different PS samples (i.e., ones from different suppliers) show reasonable agreement, better for LCS than for UCS. We ascribe the differences to sample impurity and remark that it obviously will be necessary to employ a self-consistent set of samples when studying trends with molecular weight. Some of the differences we have observed between the low- and high-precision results (compare Table II with Table I of ref 4) can be ascribed to the purification (and concomitant fractionation) carried out between the low- and high-precision measurements.[4] For the high-precision measurements we also paid more careful attention to solvent drying. Thus it is appropriate to suggest that inconsistencies between the low-precision (Table II) and high-precision data (Table I, ref 4) are due to the sum of the effects of improved polymer purity, molecular weight fractionation caused by the purification procedure, and improved solvent drying for the high-precision data.

Table III
Isotope Effects on Cloud Points for Polystyrene–$(CH_3)_2CO$ and –$(CD_3)_2CO$ Solutions[a]

sample	T_{UCS}(H), K	ΔT_{UCS}, K	T_{LCS}(H), K	ΔT_{LCS}, K	$\Delta(dT/dP)_u$[b]
PS-130	293		400		
PS-80	260	-22	437	18	
PS-55	251	-19	452	16	
PS-115	268	-22	430	22	0.5
PS-75	255	-20	442	14	0.5
PS-50	245	-16	458	14	

[a] Visual determination in sealed capillaries, $W_1' = 0.2$ (see eq 3). $\Delta T = T(H) - T(D)$. [b] $\Delta(dT/dP)_u = (dT/dP)_{upper,H} - (dT/dP)_{upper,D}$. Units are K·MPa^{-1}.

High-Precision Measurements, Light Scattering. Laser light scattering results for acetone–polystyrene solutions including a detailed discussion of our methods of data analysis are presented elsewhere.[4] In the next section results obtained from both the high- and low-precision measurements will be discussed in the context of the theory of isotope effects in condensed phases.[1,2]

Discussion

This paper and its companion[4] are the first in a series that will discuss effects of H/D substitution and pressure on phase separation in polymer solvent systems. Preliminary IE data of relatively low precision for the UCS and LCS branches of polystyrene dissolved in either acetone or methylcyclopentane and high-precision data for the UCS branch of the PS–acetone system are reported at several molecular weights. It is not our intent to subject these data to a lengthy theoretical rationalization at this time; that more appropriately awaits a broader data net over a wide range of molecular weights including both UCS and LCS branches. Still it is useful to discuss the present data in the context of condensed-phase isotope effect theory, even if that discussion is preliminary.

Cloud and Spinodal Points. The phase equilibrium data in $(CH_3)_2CO$ are self-consistent, once it is recognized that purifications carried out between the low- and high-precision measurements have resulted in significant polymer purification and/or fractionation. Thus PS-75 in $(CH_3)_2CO$ with a low-precision cloud point (LPCP) around 270 K, after purification, shows its high-precision cloud point (HPCP) 16 K lower, while PS-115, with LPCP = 272 K, displays HPCP = 248 K, 24 K lower. It is clear from MW checks that we carried out by viscosity,[49] from the small differences between CP and spinodal temperatures,[4] and from the near identity of (dT/dP),[4] all comparing PS-75 and PS-115, that the purified samples are much closer in molecular weight than indicated by the supplier's specifications in Table I. Comparisons are complicated because M_w/M_n is significantly different for the two samples. In comparing isotope effects we have been scrupulous in ensuring that identical polymer samples have been used in H- and D-labeled solvents. Therefore comparisons between LPCP and HPCP isotope effects are possible even though the isotopic differences are roughly comparable in magnitude to differences between LPCP and HPCP.

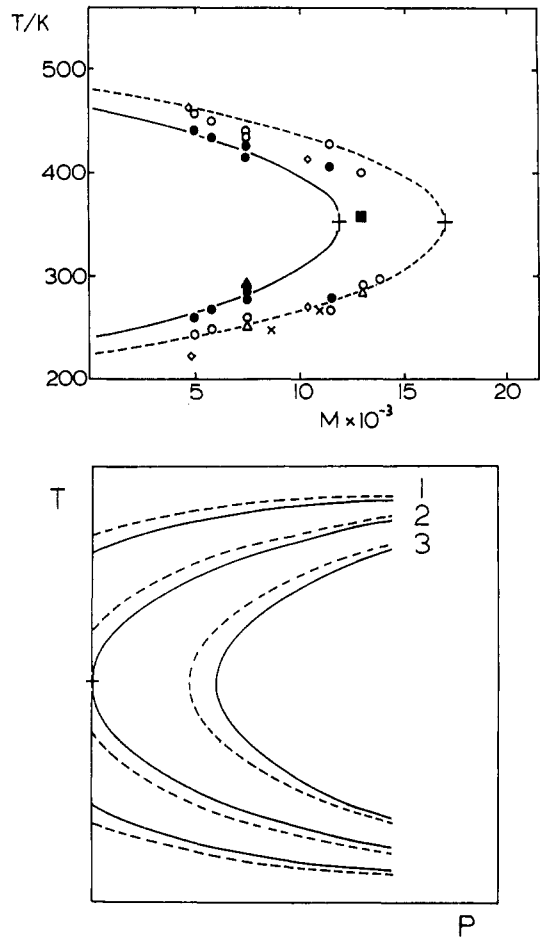

Figure 3. (a, Top) CPC maxima or minima for polystyrene–acetone solutions as a function of molecular weight at low pressure. Present CPC data, low precision in $(CH_3)_2CO$ (○); high precision in $(CH_3)_2CO$ (△) (this work and ref 4); low precision in $(CD_3)_2CO$ (●); high precision in $(CD_3)_2CO$ (▲) (this work and ref 4); Patterson and co-workers[40,41] in $(CH_3)_2CO$ (◇); Shultz and Epstein, in $(CH_3)_2CO$[50] (x); Rebelo and Van Hook, in $(CD_3)_2CO$ (■) (previously unreported). The large crosses mark the low-pressure pseudotricritical points, (M^*(H), T_c^*) and (M^*(D),T_c^*). The outer dotted curve is for solution in $(CH_3)_2CO$; the inner solid curve for solution in $(CD_3)_2CO$. The curves are correlations based on eq 5 as described in the text. At the time that correlation was made the point marked (■) was not available, presumably were it included in the correlation the predicted value of M^*(D) would increase somewhat. (b, Bottom) CP maxima or minima for polystyrene–acetone solutions as a function of pressure at several molecular weights (schematic). The cross at the center of curve 2 for MW° marks the pseudotricritical pressure, $P_c^*(MW_0)$ (see text), regarded here as a fitting parameter. For $P < P_c^*(MW_0)$ the system is in the hourglass type of phase diagram and exhibits neither UCS or LCS. The curve labeled as 2 for MW_0^*(D) (the solid line) marks the maximum PS-MW that shows both LCS and UCS in $(CD_3)_2CO$ solutions at zero pressure. For higher MW's (say curve 3) and at pressures below P_c^*(MW) (i.e., for points to the left of the origin of any parabola specified by MW > MW_0^*) the system is in the hourglass configuration but can be forced back to the UCS/LCS configuration by raising the pressure. For lower MW's (curve 1) and at pressures above $P_c^*(MW_0)$ the system can never reach the hourglass configuration unless a negative pressure is applied. It is obviously possible to adjust pressure for a given set of curves so that the H sample is in the LCS/UCS configuration, while the *D* is in the hourglass configuration. That is not possible for MW < MW_0^* (curve 3), since negative pressures would be required. (—) D; (- - -) H.

Low-pressure CP data as a function of MW are shown in Figure 3a. They are in reasonable agreement with Patterson and co-workers[40,41] and Shultz and Epstein.[50] The figure plots maxima of cloud point curves (CPC's), $T_{max,CPC}$, versus polymer molecular weight. Polydispersity displaces T_c to higher concentration (lower temperature)[51] but these CPC curves are flat and ($T_{max,CPC} - T_c$) is not large on the scale of the figure. We have chosen not to use a Shultz–Flory[52] plot because the large curvature rules out any simple interpretation. For deuterated acetone the CPC maxima are displaced 22 ± 3 K above the UCS branch and 17 ± 2 K below the LCST. The values are approximate since they stem mostly from low-precision visual CPC determinations. The high-precision scattering measurements show consistently larger isotope effects (at two molecular weights and using separately purified and dried $(CH_3)_2CO$ and $(CD_3)_2CO$). T_c's are hypersensitive to water impurity, and we conclude data from the visual CPC measurements, where the solutions were not as scrupulously handled, are of lower accuracy. Continued refinement will follow as the program progresses. Examination of Table I, ref 4, shows the cloud and spinodal points for the HP data follow each other closely, being separated by only about $^1/_2$ deg or so, even far from T_c. Although for no good reason we had expected larger differences, the observation that ($T_{cpc} - T_s$) is small is consistent with the one of Kiepen and Borchard[53] for oligomeric polystyrene in pentane (M_n = 1000; M_w/M_n = 1.1).

Both the polymer molecular weight and the pressure dependences of the phase diagrams are outlined in Figure 3. In Figure 3a for molecular weights on the right-hand side of the diagram (i.e., greater than the hypercritical value, which is marked with a large cross), the system has made its transition from a "maximum–minimum" to an "hourglass" shape and no longer displays UCS or LCS demixing. In the simplest analysis, i.e., a monodisperse polymer solute with $T_{max,CPC} = T_{c,UCS}$ and $T_{min,CPC} = T_{c,LCS}$ and with $\xi_{c,UCS}$ and $\xi_{c,LCS}$ showing an identical M_1 dependence, the hypertransition point (cross) would be a tricritical point, were tricritical points not forbidden by the phase rule for systems of fewer than three components.[54] In the present case, CPC maxima or minima do not coincide with T_c, so even though tricritical points are allowed (there are more than three components), it is inaccurate to label the intersection of the ($T_{max,CPC}$,M)$_{UCS}$ and ($T_{min,CPC}$,M)$_{LCS}$ curves a tricritical point. Still ($T_{max,CPC} - T_c$)$_{UCS}$ and presumably ($T_{min,CPC} - T_c$)$_{LCS}$ are small, and a simplified treatment seems warranted. In that treatment we label the points of intersection (crosses), marking the (UCS/LCS ↔ hourglass) transition "pseudotricritical points". Thermodynamics reveals that tricritical points do not occur at a cusp. The path joining LCS and UCS must be rounded as shown schematically in Figure 3a (dotted lines). The correlation is based on the analysis below, which following Knobler and coworkers[28,54] assumes a 0.5 power law.

$$|T_c^* - T_c| = b(M^* - M)^{1/2} \qquad (5)$$

T_c^* is the tricritical temperature and M^* the corresponding molecular weight. Initial fits to the $(CH_3)_2CO$ and $(CD_3)_2CO$ data showed $T_c^*(H) \cong T_c^*(D)$. The least squares result (plotted as the dotted lines, Figure 3a) obtained upon setting $T_c^*(H) = T_c^*(D) = T_c^*$ and $b_H = b_D = b$ and using $M^*_{1,D} = 12 \times 10^3$ and $M^*_{1,H} = 17 \times 10^3$ obtained from analysis of the solubility (see next section), yields T_c^* = 353 K and b = 1.026 as best values for a two-parameter least squares fit. The presently available data are neither extensive nor precise enough to permit extraction of all four parameters (b, T_c^*, $M^*_{1,d}$, $M^*_{1,h}$) by least squares.

Mean Field Analysis, Cloud Point Data. A mean field treatment of CPC data, expanding on the work of Prigogine and Defay,[38] follows. Writing free energy as a

function of temperature, pressure, polymer concentration and molecular weight, and solvent isotope content, D/H, $G = G(T,P,\xi,M,\mathrm{D/H})$, and recognizing at either $T_{c,UCS}$ or $T_{c,LCS}$ $\partial^2G/\partial\xi^2 = \partial^3G/\partial\xi^3 = 0$ and $\partial^4G/\partial\xi^4 > 0$, we have for a perturbation along the critical line

$$\delta(\mathrm{d}^2G/\mathrm{d}\xi^2)_c = 0 = (\partial^3G/\partial\xi^2\,\mathrm{d}P)_c\delta P + (\partial^3G/\partial\xi^2\partial T)_c\delta T + (\partial^3G/\partial\xi^2\partial M)_c\delta M + (\partial^3G/\partial\xi^2\partial(\mathrm{D/H}))_c\delta(\mathrm{D/H}) \quad (6)$$

Here ξ is an appropriate concentration variable. In writing a relation such as eq 6 we assume the free energy is a continuous and differentiable function of M and D/H, just as it is for P and T. This is reasonable for D/H because the chemical nature of the system does not change with isotope enrichment, the PES describing the system is isotope independent and consequently G should vary smoothly between extrema of this parameter. For the M dependence the picture is not as clear. M can only change in discrete single monomer units so the (G,M) surface is not continuous. Even so differences between successive oligomers are small relative to solute–solvent differences. Thus properties like volume per monomer unit, bond moments, and force constants appear to be transferrable from oligomer to oligomer with high accuracy.[55] It therefore seems reasonable to approximate the (G,M) surface as continuous with respect to the M variable. The assumption leads straightforwardly to a continuous thermodynamics for polymer–polymer and polymer–solvent mixtures. Ratsch and co-workers[56] have developed such a continuous thermodynamics for polymers, and it is in that same spirit that eq 6 and the analysis below are offered. Referring again to eq 6 we find at constant M and D/H the pressure coefficient is

$$(\mathrm{d}T/\mathrm{d}P)_{c,M,\mathrm{D/H}} = -(\partial^3G/\partial\xi^2\partial P)_c/(\partial^3G/\partial\xi^2\partial T)_c = (\partial^2V/\partial\xi^2)_c/(\partial^2S/\partial\xi^2)_c \quad (7)$$

S is the entropy and V the volume of the mixture. At constant P and D/H the M dependence is, similarly

$$(\mathrm{d}T/\mathrm{d}M)_{c,P,\mathrm{D/H}} = -(\partial^3G/\partial\xi^2\partial M)_c/(\partial^3G/\partial\xi^2\partial T)_c = (\partial^2(\partial G/\partial M)/\partial\xi^2)_c/(\partial^2S/\partial\xi^2)_c \quad (8)$$

and at constant P and M the D/H dependence is

$$(\mathrm{d}T/\mathrm{d}(\mathrm{D/H}))_{c,P,M} = -(\partial^3G/\partial\xi^2\partial(\mathrm{D/H}))_c/(\partial^3G/\partial\xi^2\partial T)_c = (\partial^2(\partial G/\partial(\mathrm{D/H}))/\partial\xi^2)_c/(\partial^2S/\partial\xi^2)_c \quad (9)$$

From eq 7 at values of M below the pseudotricritical point, we obtain $\partial^2S/\partial\xi^2 < 0$, with $(\mathrm{d}T/\mathrm{d}P)_c$ of the opposite sign to $\partial^2V/\partial\xi^2$ for the UCS branch,[38] and $\partial^2S/\partial\xi^2 > 0$, with $(\mathrm{d}T/\mathrm{d}P)_c$ of the same sign as $\partial^2V/\partial\xi^2$ for the LCS branch. In the present case $(\mathrm{d}T/\mathrm{d}P)_c$ is positive for the LCS branch and negative for UCS. We conclude $\partial^2V/\partial\xi^2 > 0$ along both branches. The shape of the T,P diagram (Figure 3b) is thus primarily controlled by the pressure dependence of the curvature of the entropy, $(\partial^2S/\partial\xi^2)$, which goes through zero at the pseudotricritical point. The smooth (and in the limit infinite) curvature near the pseudotricritical point follows if one recognizes $(\partial/\partial^2S/\partial\xi^2)/\partial P)_M$ is smoothly varying as it goes through its zero.

To analyze the M dependence of T_c note that eq 8 is pseudothermodynamic and assumes continuity of state with polymer molecular weight. That accepted, we have from the data $(\mathrm{d}T/\mathrm{d}M)_{c,P} < 0$ for LCS where $\partial^2S/\partial\xi^2 > 0$ and conclude $\partial^2(\partial G/\partial M)_{c,P}/\partial\xi^2 < 0$. For UCS $(\mathrm{d}T/\mathrm{d}M)_{c,P} > 0$ and $\partial^2S/\partial\xi^2 < 0$, again $\partial^2(\partial G/\partial M)_{c,P}/\partial\xi^2 < 0$. Again, the shape of the diagram is primarily controlled by the contribution of the entropic term, as it is in eq 9, which describes curvature along the critical line as D/H is changed.

Knobler and co-workers[28,54] have commented on the approach to the tricritical point, noting that curvature is consistent with an extended classical mean field theory. The apparatus and techniques described in this paper could be usefully employed to further examine this point. Detailed study in the (T,M) plane would be laborious and very likely imprecise, since it necessitates preparation of a series of polymers at closely spaced molecular weight. Errors are to be expected from slightly different molecular weight distributions and/or impurities, sample to sample. However, the present methods are well adapted for studying curvature in the (T,P) or $(T,\mathrm{D/H})$ planes for samples of appropriate molecular weight (near the pseudotricritical point). We are currently engaged in such measurements.

We conclude this section with further discussion of the correlations in Figure 3a. For deuterio solutions around 300 K we observed solubility at M = 11 500 but not at M = 13 000. For protioacetone we found solution at M = 13 000 as did Shultz and Epstein[50] at 14 000 (with as yet no significant departure from the approximately linear part of the correlation line, Figure 3a). Siow et al.[40] report the system had coalesced to the hourglass shape by M = 19 800 but state they are "obviously very close to showing both UCS and LCS". A more precise definition of that value of M defining the zero-pressure pseudotricritical point awaits more data; for now we take $M^*_{1,D}(P=0)$ = 12 000 ± 500 and $M^*_{1,H}(P=0)$ = 17 000 ± 2000.

It is interesting to consider the effects of pressure, M_1, and solvent D/H content from a slightly different point of view. The admittedly inadequate first-order Flory–Huggins or Guggenheim solution theories lead straightforwardly to the prediction that for solutions with an excess free energy surface, $G^{ex} = \xi(1-\xi)\chi$, the system crosses from one to two phases at $T_c = \chi/2R$. In general χ may be a function of concentration, temperature, pressure, solute molecular weight, solvent, D/H substitution, etc., $\chi = \chi(T,P,\xi,M,\mathrm{D/H},...)$, and this is one well-established mechanism by which an extended theory can be developed. In this context it is instructive to draw the phase diagram[57] in the $(\chi/2R,T)$ plane (Figure 4a). The two-phase region lies above the diagonal, the one-phase region below. The case of interest occurs when $(\mathrm{d}^2(\chi/2R)/\mathrm{d}T^2)$ is positive and the magnitude of $(\chi/2R)$ is such that it cuts the diagonal at two points, as shown in the figure, giving rise to LCS and UCS branches. Various functional forms are possible, a simple one is

$$\chi/2R = \chi_0(P,\xi,M,...)/2R + (\chi_1(P,\xi,M,...)/2R)T + (\chi_2(P,\xi,M,...)/2R)T^2 \quad (10a)$$

$$G^e = (\xi - \xi^2)\chi \quad (10b)$$

The effects of varying M, P, and solvent D/H ratio are shown schematically in Figure 4. Unfortunately the two points of intersection at UCS and LCS obtained by examination of the phase diagrams do not furnish enough information to define all three parameters in eq 10, nor do the M, P, or D/H dependences of the T_c's give sufficient information to completely define the various derivatives, $\partial\chi_0/\partial M$, $\partial\chi_1/\mathrm{d}M$, ..., $\partial\chi_0/\partial P$, ..., $\partial\chi_2/\partial(\mathrm{D/H})$.

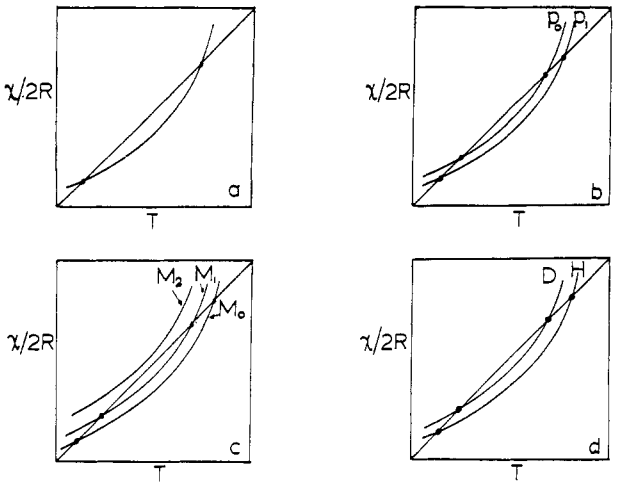

Figure 4. (a) Phase diagrams in the $(\chi/2R,T)$ plane, schematic. The two-phase region lies above the diagonal; phase separation of the UCS and LCS types is found below and above the points of intersection with the diagonal. (b, c, and d) Effects of pressure, molecular weight, and solvent D/H content, respectively. The cases diagrammed are those consistent with the PS–acetone system. The miscibility gap is widened by decreasing the molecular weight ($M_0 < M_1 < M_2$), increasing the pressure ($P_0 < P_1$), or decreasing the D/H ratio in the solvent.

Isotope Effects on T_c(UCS). Symmetrical Mixture Theory. In this section we formulate the essentials of a simple physical interpretation of isotopic differences, $\Delta T_c = T_c(H) - T_c(D)$. The approach applies the two-parameter symmetrical mixture theory (SMT) of Guggenheim,[35] as modified for interpretation of condensed-phase isotope effects by Singh and Van Hook.[22] SMT, which makes no attempt to treat the effects of polydispersity, is strictly applicable only to those solutions with spinodal and binodal curves symmetric with respect to the concentration variable and with maxima at $\xi_c = 0.5$. Although application to the present problem will be at best approximate, we anticipate that SMT will usefully describe the physical origins of demixing. By minimizing the number of parameters in the theory we hope to focus on the isotope effects in the clearest possible fashion.

Consider, for example, the data on PS-75 reported in Table I, ref 4, and shown in Figure 5a,b. The demixing curves in the (T,φ) planes are markedly skewed with maxima at $\varphi_h = \varphi_d = 0.15$. The effect of dispersity is apparent. The CPC maxima and T_c do not coincide. The local dip in CPC observed in the vicinity of T_c is of interest. Similar behavior has been widely seen in other polydisperse solutions.[6,58] For the solution in $(CH_3)_2CO$ the shape of the CPC/T curve is in excellent agreement with that reported by Van der Haegen et al.[59] for c-C_6H_{12} solutions of a very similar polystyrene (M_w/M_n also equal 1.07). The agreement extends to observation of the local dip near T_c. The CPC's show large isotope effects, $\Delta T_{max} = (T_{max,CPC,H} - T_{max,CPC,D}) = -32.1$ K.

Introducing approximations leading to SMT, we ignore the complications discussed above and change from the φ scale to a second volume-based concentration scale, denoted as the ψ scale. Consider the solutions as pseudobinary mixtures of $V_{PS}°$ volumes of PS with $7.75V°_{acetone}$ volumes of $(CH_3)_2CO$ or $(CD_3)_2CO$. The ratio corresponds to that at $T \sim T_c$. $V_{PS}°$ and $V_{acetone}°$ are standard-state partial molar volumes of liquid $C_6H_5CHCH_2$ monomer segment,[46] vide supra, and acetone, respectively (i.e., a mixture of 1 mol of PS-75 monomer per 7.75 mol of acetone shows $\psi_1 = 0.5$). Weight/weight concentrations were converted to φ and thence to the ψ_{PS} scale by using the specific volumes of Hoecker et al.[46] for polystyrene and

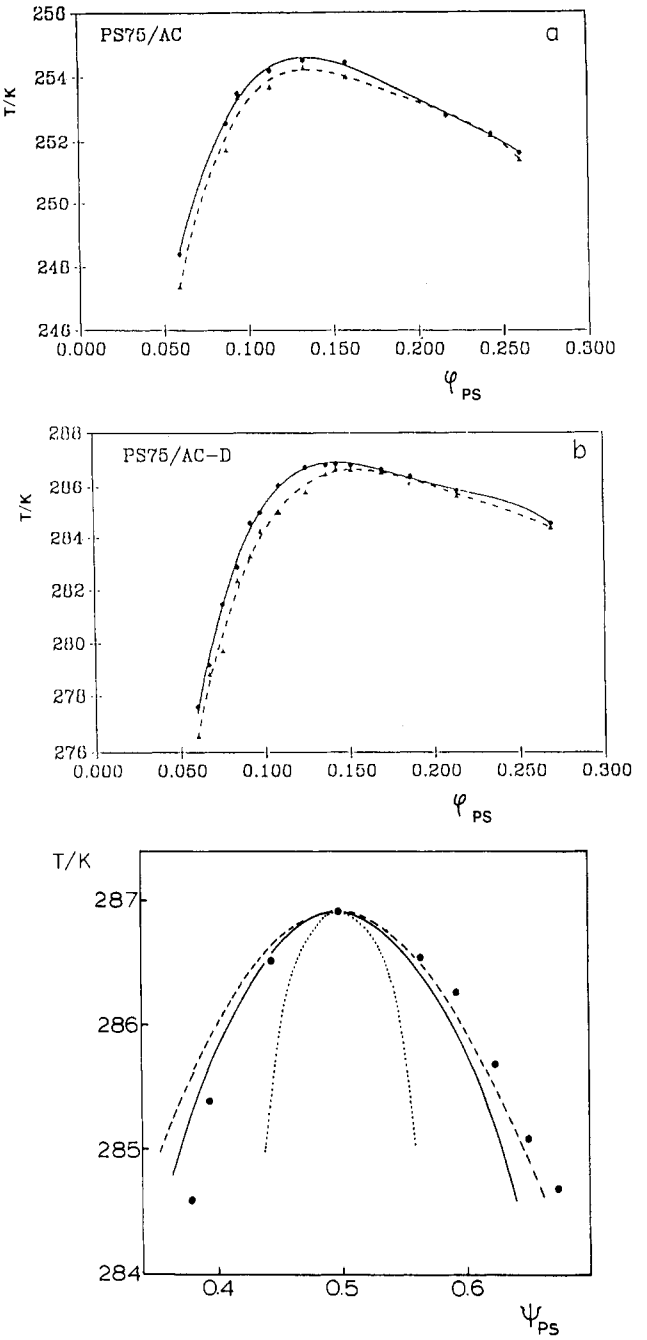

Figure 5. (a) Cloud and spinodal loci for polystyrene (MW = 7500, Table I) –$(CH_3)_2CO$ solutions. The data are from ref 4, Table I, and are of the type labeled high precision in this paper. (b) Same as part a except the solvent is $(CD_3)_2CO$. (c, Bottom) UCS cloud point loci for PS-75–$(CD_3)_2CO$ solutions (part b) using the ψ_{PS} concentration scale (ψ_{PS} = (mol of PS)/(mol of PS + mol of acetone)/7.75). The data are much more nearly symmetric when plotted in the ψ_{PS} scale than in the ψ_V scale, compare above. The solid dots are picked from the experimental CPC's. The lines are calculated as described in the text from $T_c(D) = 286.9$ and various values for z: (···) $z = \infty$; (—) $z = 6$; (- - -) $z = 5$. The fit is sufficiently good to warrant extension of the theory to the treatment of isotope effects.

Kooner and Van Hook[60] for $(CH_3)_2CO$ and $(CD_3)_2CO$. Figure 5c demonstrates demixing is very nearly symmetrical for the ψ_{PS} scale, although it is highly unsymmetrical when plotted in the φ or W' scales (cf. Figure 5a,b). Equation 11 expresses the SMT excess free energy as a function of ψ. Here z is the coordination number in the

$$G^e = (\psi - \psi^2)[B_g - B_g^2(\psi - \psi^2)/(zRT) + ...] \quad (11)$$

pseudolattice defining the statistical problem, and B_g is

the partial molar free energy of transfer from the pure reference liquid to infinitely dilute solution in the other component, $B_g = B_g(T,P,D/H, ...)$. B_g, like χ (above), is a parameter defining the excess free energy, but eq 11 is of a more specific form than eq 10 and involves fewer parameters. From eq 11 the binodal locus is defined

$$\ln(\psi'/\psi'') = B_g(\psi' - \psi'') + (B_g^2/(zRT))((\psi' - \psi'') - 3(\psi'^2 - \psi''^2) + 2(\psi'^3 - \psi''^3)) \quad (12)$$

ψ' and ψ'' are the concentrations of the coexisting phases. For $\psi_c = 0.5$, $T_c = B_g m_z/(4R)$ with $m_z = 1 + (1 - 4/z)^{1/2}$. The expression reduces to that for a strictly regular solution at $z = \infty$, where $B_g(\text{st reg}) = 2RT_c$. To model the D/H effect, z and m_z are taken as independent of isotope, so

$$\Delta T_c/T_c = (\Delta B_g/B_g)((zm_z - 4)/(zm_z - 2)) = (\delta\Delta\mu_0^\infty/\delta\mu_0^\infty)\Omega' \quad (13)$$

Ω' is defined in the equation and $\delta\Delta\mu_0^\infty = (\mu^\infty - \mu^\circ)_H - (\mu^\infty - \mu^\circ)_D$. The superscript "$\infty$" refers to infinite dilution, "$\circ$" to the pure reference state. The solutions are symmetric, so for each isotope $\delta\mu_0^\infty(1) = \delta\mu_0^\infty(2)$. Note carefully, however, the transfers are not at the same temperatures for the H and D solutions but occur at $T_c(H)$ and $T_c(D)$, respectively. To compare at a single temperature, say $T_c(D)$, one can write

$$\Delta\mu_0^\infty(T_c(D)) = \mu_0^\infty(H,T_c(D)) - \mu_0^\infty(D,T_c(D)) = \mu_0^\infty(H,T_c(H)) - \mu_0^\infty(D,T_c(D)) + \int (\partial\mu_0^\infty(H)/\partial T)\, dT \quad (14)$$

The integral extends from $T_c(H)$ to $T_c(D)$. Numerical evaluation awaits data on the enthalpies or entropies of transfer or an independent determination of μ_0^∞; neither is yet available for acetone solutions. Some bounding, however, is possible. For the present case, $T_c(LCS) > T_c(UCS)$, so χ_0 and χ_2 (eq 10) are necessarily greater than zero (arguing from the shape of the diagram and the form of eq 10). If in trial fits one changes χ_0/T over the range $0 < \chi_0/T < 2$ and uses $T_c(LCS)$ and $T_c(UCS)$, then CORR $(\Delta\mu_0^\infty) = \int(\partial\mu_0^\infty(H)/\partial T)\, dT/(\mu_0^\infty(H,T_c(H)) - \mu_0^\infty(D,T_c(D))$ drops smoothly from 1 to 0. Thus from eq 14 at $\chi_0/T = 0$, $\Delta\mu_0^\infty(T_c(D)) = 0$, while at the upper bound, $\chi_0/T = 2$, $\Delta\mu_0^\infty(T_c(D)) = \mu_0^\infty(H,T_c(H)) - \mu_0^\infty(D,T_c(D))$, i.e., just that value calculated by assuming a temperature-independent free energy. It is not likely that $\chi_0/T > 2$ in the vicinity of the phase transition, and it is impossible that it be less than zero. Although independent free energy or enthalpy data are not available for acetone, Flory and Hoecker[61] have analyzed the polystyrene–methyl ethyl ketone system finding a reduced residual chemical potential of about 0.5. This is equivalent to CORR $(\Delta\mu_0^\infty) = 0.8$, or $\delta\Delta\mu_0^\infty/\Delta\mu_0^\infty = 0.2(\Delta T_c/T_c)$. The calculation is meant only to point out the importance of the correction and roughly approximate it.

Application. We have applied eq 11–14 to interpret data for isotope effects on demixing and illustrate that process with a discussion of acetone–PS-75 solutions. Using $T_c(H) = 254.6$ K, $T_c(D) = 286.9$, and $z = 6$ (nearest whole number), eq 12 reproduces the concentration dependence of the demixing to reasonable approximation although some residual skewing remains apparent. Figure 5c compares experimental data for PS–$(CH_3)_2CO$ with the calculated curves for $z = \infty$ (the strictly regular result), $z = 6$, and $z = 5$. The fits are good enough to conclude that extension to the treatment of isotope effects is warranted. For PS-75,[4] $\Delta T_c/T_c = 0.113$, so $\delta\Delta\mu_0^\infty/RT = 0.391$. This is the isotope effect for the transfer of 7.75 mol of acetone from the Raoult's law pure liquid standard state to the Henry's law infinite dilution standard state (in PS-75 "liquid"), the two solutions at temperatures $T_c(H)$ and $T_c(D)$. Using, very approximately, the correction estimated in the section following eq 14, the isotope effect on the free energy of transfer per deuterium is $(\delta\Delta\mu_0^\infty(T_{CPC,max}(D))/RT)_{per\ D} = 0.2 \times 0.391/(7.75 \times 6) = 1.7 \times 10^{-3}$.

The Connection with Molecular Properties. A common approximation used in qualitative or semiquantitative discussions of condensed-phase isotope effects is the Bigeleisen[1] AB equation[1,2,22]

$$\delta\Delta\mu_0^\infty/RT = A/T^2 + B/T \quad (15a)$$

$$A = (1/24)(hc/k)^2\Sigma_i(\nu_i'^2 - \nu_i^2)^\infty - (\nu_i'^2 - \nu_i^2)^\circ \quad (15b)$$

$$B = (1/2)(hc/k)\Sigma_j(\nu_j' - \nu_j)^\infty - (\nu_j' - \nu_j)^\circ \quad (15c)$$

In these equations h is Planck's constant, c is the velocity of light, and k is Boltzmann's constant. The prime designates the lighter isotope, and the equation is written for the case where the vibrational frequencies (cm^{-1}) of the molecule of interest (acetone in our case) fall neatly into two classes, a high-frequency set (indexed over j), which can be treated in the zero-point energy approximation (the B term) and a low-frequency set (indexed over i), which includes the external vibrations and librations and the internal rotations and which is to be treated in the high-temperature approximation (the A term). Also $(i_{max} + j_{max}) = 3n$, where n is the number of atoms in the molecule under consideration. From detailed information on the temperature coefficient of the isotope effect (not yet available) the relative contributions of the A and B terms can be calculated. The IE on reduced free energy of transfer of acetone from liquid to vapor (vapor pressure isotope effect, VPIE) has important contributions from both A and B in this temperature range. That is established by the data of Kooner and Van Hook[60] who report a maximum in $\ln(P'/P) = \delta\Delta\mu_{liq}^{vap}/RT$ at $T = 334$ K. Similarly one expects both "A" and "B" contributions to the transfer free energy isotope effects in solution. A detailed analysis awaits extensive data on temperature dependence but the extremes of possible A and B contributions are defined by the present observations. Were the IE completely due to a zero-point energy effect (B term, an effect most reasonably accounted for by a frequency shift in the CH/CD stretching modes on phase change), then $(\delta\Delta\mu_0^\infty(T_c(D))/RT)_{per\ D}$ would be equivalent to a 2-cm^{-1} blue shift in the CH stretching frequency of acetone on the transfer from the acetone-rich to the polystyrene-rich phase. Any A contribution from the low-frequency motions (say from shifts in the internal or external rotational frequencies, which are more isotope sensitive than are the hindered translations) will compensate for part of the zero-point energy shift. For the moment we note that a shift on the order of 2 cm^{-1}, when an acetone molecule is transferred from the pure liquid to infinite dilution in PS, serves to rationalize the UCS demixing isotope effect. Typical zero-point energy shifts on the transfer of van der Waals bonded fluids from the dilute gas to the liquid state are on the order of 8–12 cm^{-1}, so the magnitude of the calculated shifts is reasonable. Although each polymer segment interacts with a large number of solvent vibrational modes, each individual interaction is of a modest scale. The symmetric mixture analysis for the concentration dependence of the free energy (eq 12) and for the isotope effects (eq 14 and 15) is consistent with the idea that the fundamental interaction in the

solution is one involving a large number of solvent molecules with each monomer segment.

Conclusion

Experiments setting forth the isotope and pressure dependences of demixing in polystyrene–solvent systems are reported. The results in $(CH_3)_2CO$ and $(CD_3)_2CO$ solvents have been analyzed in the context of the theory of isotope effects in condensed phases. The analysis, limited in this paper to the use of a pseudobinary model with coincident spinodal and binodal maxima at critical conditions, demonstrates participation of a large number of solvent molecules (≈7.8 for PS-7500) with each monomer segment. As more data becomes available it will become possible to refine the model to include the effect of MW dispersion. In the context of the present model the solvent–monomer interaction is equivalent to an $\sim 2\text{-cm}^{-1}$ ZPE blue shift per CH/CD acetone oscillator on transfer from pure solvent to highly dilute solution in polystyrene.

Acknowledgment. This work was supported by the U.S. Department of Energy, Division of Materials Sciences, under Grant 88ER45374.

References and Notes

(1) Bigeleisen, J. *J. Chem. Phys.* **1961**, *34*, 1485.
(2) Jancso, G.; Van Hook, W. A. *Chem. Rev.* **1974**, *74*, 689.
(3) Prausnitz, J. M. *Molecular Thermodynamics of Fluid Phase Equilibria*; Prentice-Hall: Englewood Cliffs, NJ, 1969.
(4) Szydlowski, J.; Rebelo, L. P.; Van Hook, W. A. *Rev. Sci. Instrum.*, in press.
(5) Wignall, G. D. In *Neutron Scattering from Polymers*, in *Encyclopedia of Polymer Science and Engineering*; Grayson, M., Kroschwitz, J., Eds.; John Wiley and Sons: New York, 1987.
(6) Olabisi, O.; Robeson, L. M.; Shaw, M. T. *Polymer–Polymer Miscibility*; Academic Press: New York, 1979.
(7) Fisher, E. W. *IUPAC 27th Int. Symp. Macromol.*; Strasbourg, 1981. Pergamon Press: New York, **1982**; p 191.
(8) Walsh, D. J.; Higgins, J. S.; Maconnachie, A. *Polymer Blends and Mixtures*; NATO ASI Series; Martinus Nijhoff, Pub.: Dordrecht, The Netherlands, 1985.
(9) Strazielle, C.; Benoit, H. *Macromolecules* **1975**, *8*, 203.
(10) Schmitt, B. J.; Kirste, R. G.; Jelenic, J. *Makromol. Chem.* **1980**, *181*, 1655. Kirste, R. G.; Lehnen, B. R. *Makromol. Chem.* **1976**, *177*, 1137.
(11) Yang, H.; Hadziioannou, G.; Stein, R. S. *J. Polym. Sci., Polym. Phys. Ed.* **1983**, *21*, 159. Yang, H.; Shibayama, M.; Stein, R. S.; Shimizu, N.; Hashimoto, T. *Macromolecules* **1986**, *19*, 1667.
(12) Atkin, E. A.; Kleintjens, L. A.; Koningsveld, R.; Fetters, L. J. *Makromol. Chem.* **1984**, *185*, 377. Atkin, E. A.; Kleintjens, L. A.; Koningsveld, R.; Fetters, L. J. *Polym. Bull.* **1982**, *8*, 347.
(13) Lin, J. L.; Rigby, D.; Roe, R. J. *Macromolecules* **1985**, *18*, 1609.
(14) Bates, F. S.; Wignall, G. D. *Macromolecules* **1986**, *19*, 932.
(15) Bates, F. S.; Wignall, G. D.; Koehler, W. C. *Phys. Rev. Lett.* **1985**, *55*, 2425. Bates, F. S.; Dierker, S. B.; Wignall, G. D. *Macromolecules* **1986**, *19*, 1938. Bates, F. S.; Wignall, G. D. *Phys. Rev. Lett.* **1986**, *57*, 1429.
(16) Bates, F. S.; Muthukumar, M.; Wignall, G. D.; Fetters, L. J. *J. Chem. Phys.* **1988**, *89*, 535.
(17) Singh, R. R.; Van Hook, W. A. *Macromolecules* **1987**, *20*, 1855.
(18) Singh, R. R.; Van Hook, W. A. *J. Chem. Phys.* **1987**, *86*, 2969.
(19) Prigogine, I. *The Molecular Theory of Solutions*; North-Holland Publ.: Amsterdam, 1957.
(20) Rabinovitch, I. B. *Influence of Isotopy on the Physicochemical Properties of Liquids*; Consultants Bureau: New York, 1970.
(21) Khurma, J. R.; Kooner, Z. S.; Fenby, D. *Fluid Phase Equilib.* **1981**, *7*, 327.
(22) Singh, R. R.; Van Hook, W. A. *J. Chem. Phys.* **1987**, *87*, 6097.
(23) Salvi, M.; Van Hook, W. A. *J. Phys. Chem.* **1990**, *94*, 7812.
(24) Stanley, H. E. *Introduction to Phase Transitions and Critical Phenomena*; Oxford University Press: Oxford, 1971. Scott, R. L. *Specialist Periodical Reports, Chemical Thermodynamics*; The Chemical Society: London, 1978; Vol. 2, p 238. Domb, C. *Contemp. Phys.*, **1985**, *26*, 49.
(25) Gordon, M.; Torkington, J. A. *Pure Appl. Chem.* **1981**, *53*, 1461.
(26) Singh, R. R.; Van Hook, W. A. *J. Chem. Phys.* **1987**, *87*, 6088.
(27) Levelt-Sengers, J. M. H.; Sengers, J. V. *Perspect. Stat. Phys.* **1981**, *9*, 239. Chen, Z.-Y. Crossover from singular critical to regular classical behavior. Thesis, University Maryland, 1988.
(28) Shen, W.; Smith, G. R.; Knobler, C. M.; Scott, R. L. *J. Phys. Chem.* **1990**, *94*, 7943. Pegg, I.; Knobler, C. M.; Scott, R. L. *J. Chem. Phys.* **1990**, *92*, 5442. Scott, R. L. *Acc. Chem. Res.* **1987**, *20*, 97.
(29) De Pablo, J.; Prausnitz, J. M. *Fluid Phase Equilib.* **1990**, *59*, 1.
(30) Carvoli, G.; Castelli, A.; Marconi, A. M. *Fluid Phase Equilib.* **1990**, *56*, 257.
(31) Stroeks, A.; Nies, E. *Macromolecules* **1990**, *23*, 4088, 4092.
(32) Koningsveld, R.; Stockmayer, W. H.; Kennedy, J. W.; Kleintjens, L. A. *Macromolecules* **1974**, *7*, 73.
(33) Irvine, P.; Gordon, M. *Macromolecules* **1980**, *13*, 761.
(34) Sanchez, I. *J. Appl. Phys.* **1985**, 2871. Dobishi, T.; Nakata, M.; Kaneko, K. *J. Chem. Phys.* **1980**, *72*, 6685, 6692; **1984**, *80*, 948.
(35) Guggenheim, E. A. *Applications of Statistical Mechanics*; Clarendon Press: Oxford, 1966.
(36) Sanchez, I. C. *Encycl. Phys. Sci. Technol.* **1987**, *11*.
(37) Solc, K. *Macromolecules* **1986**, *19*, 1166; **1987**, *20*, 2506. Solc, K.; Kleintjens, L. A.; Koningsveld, R. *Macromolecules* **1984**, *17*, 573.
(38) Prigogine, I.; Defay, R. *Chemical Thermodynamics*; Everett, D., translator; Longmans: London, 1954; Chapter, 16.
(39) Van Hook, W. A. *J. Chem. Phys.* **1985**, *83*, 4107.
(40) Siow, K. S.; Delmas, G.; Patterson, D. *Macromolecules* **1972**, *5*, 29.
(41) Zeman, L.; Patterson, D. *J. Phys. Chem.* **1972**, *76*, 1214.
(42) Saeki, S.; Kuwahara, N.; Hamano, K.; Kenmochi, Y.; Yamaguchi, T. *Macromolecules* **1986**, *19*, 2353.
(43) Flory, P. J.; Orwell, R. A.; Vrij, A. *J. Am. Chem. Soc.* **1964**, *86*, 3507. Flory, P. J. *J. Am. Chem. Soc.* **1965**, *87*, 1833.
(44) Patterson, D.; Delmas, G. *Trans. Faraday Soc.* **1969**, *65*, 708.
(45) Ye, Y.; Van Hook, W. A., unpublished results.
(46) Hoecker, H.; Blake, G. J.; Flory, P. J. *Trans. Faraday Soc.* **1971**, *67*, 2251.
(47) Chan, T. C.; Van Hook, W. A. *J. Chem. Thermodyn.* **1975**, *7*, 1119.
(48) Singh, R. R.; Van Hook, W. A. *J. Chem. Thermodyn.* **1986**, *18*, 1021.
(49) Ye, Y.; Van Hook, W. A.; unpublished data.
(50) Shultz, A. R.; Epstein, B. N., unpublished results, 1955, as quoted in ref 40.
(51) Koningsveld, R. *Discuss. Faraday Soc.* **1970**, *49*, 180.
(52) Shultz, A. R.; Flory, P. J. *J. Am. Chem. Soc.* **1952**, *74*, 4760.
(53) Kiepen, F.; Borchard, W. *Macromolecules* **1988**, *21*, 1784.
(54) Creek, J. L.; Knobler, C. M.; Scott, R. L. *J. Chem. Phys.* **1981**, *74*, 3489.
(55) Siesler, H. W.; Holland-Moritz, K. *Infrared and Raman Spectroscopy of Polymers*; Marcel Dekker: New York, 1980.
(56) Ratzsch, M.; Kehlen, H. *Prog. Polym. Sci.* **1989**, *14*, 1.
(57) Oonk, H. A. J. *Phase Theory*; Elsevier: Amsterdam, 1981.
(58) Koningsveld, R. *Pure Appl. Chem.* **1989**, *61*, 1051.
(59) Van der Haegen, R.; Kleintjens, L. A.; Van Opstal, L.; Koningsveld, R. *Pure Appl. Chem.* **1989**, *61*, 159.
(60) Kooner, Z. S.; Van Hook, W. A. *J. Phys. Chem.* **1988**, *92*, 6414.
(61) Flory, P. J.; Hoecker, H. *Trans. Faraday Soc.* **1971**, *67*, 2258.

Registry No. PS (homopolymer), 9003-53-6; acetone, 67-64-1; methylcyclopentane, 96-37-7.